Physiologia Plantarum
An International Journal for Plant Biology

Physiologia Plantarum 155: 338–354. 2015
© 2015 Scandinavian Plant Physiology Society, ISSN 0031-9317

Nitrogen assimilation and transpiration: key processes conditioning responsiveness of wheat to elevated [CO_2] and temperature

Iván Jauregui[a], Ricardo Aroca[b], María Garnica[c], Ángel M. Zamarreño[c], José M. García-Mina[c], Maria D. Serret[d], Martin Parry[e], Juan J. Irigoyen[f] and Iker Aranjuelo[g,h*]

[a]Dpto. Ciencias del Medio Natural, Universidad Pública de Navarra, Campus de Arrosadía, E-31192 Mutilva Baja, Spain
[b]Departamento de Microbiología del Suelo y Sistemas Simbióticos, Estación Experimental del Zaidín (CSIC), Profesor Albareda 1, E-18008 Granada, Spain
[c]R&D Department, CIPAV-Timac Agro Roullier Group, Orcoyen, E-31160 Navarra, Spain
[d]Departament de Biologia Vegetal. Facultat de Biologia, Universidad de Barcelona, Av. Diagonal, 645, E-08028 Barcelona, Spain
[e]Plant Biology and Crop Science, Rothamsted Research, Harpenden, Herts, AL5 2JQ, UK
[f]Grupo de Fisiología del Estrés en Plantas (Dpto. de Biología Ambiental), Unidad Asociada al CSIC, EEAD, Zaragoza e ICVV, Logroño, Facultades de Ciencias y Farmacia, Universidad de Navarra, Irunlarrea 1, E-31008 Pamplona, Spain
[g]Department of Plant Biology and Ecology, Faculty of Science and Technology, University of Basque Country (UPV-EHU), Apdo. 644, Bilbao, E-48080 Bizkaia, Spain
[h]Instituto de Agrobiotecnología (IdAB), Universidad Pública de Navarra-CSIC-Gobierno de Navarra, Campus de Arrosadía, E-31192-Mutilva Baja, Spain

Correspondence
*Corresponding author,
e-mail: iker.aranjuelo@gmail.com

Received 17 December 2014;
revised 12 March 2015

doi:10.1111/ppl.12345

Although climate scenarios have predicted an increase in [CO_2] and temperature conditions, to date few experiments have focused on the interaction of [CO_2] and temperature effects in wheat development. Recent evidence suggests that photosynthetic acclimation is linked to the photorespiration and N assimilation inhibition of plants exposed to elevated CO_2. The main goal of this study was to analyze the effect of interacting [CO_2] and temperature on leaf photorespiration, C/N metabolism and N transport in wheat plants exposed to elevated [CO_2] and temperature conditions. For this purpose, wheat plants were exposed to elevated [CO_2] (400 vs 700 μmol mol^{-1}) and temperature (ambient vs ambient + 4°C) in CO_2 gradient greenhouses during the entire life cycle. Although at the agronomic level, elevated temperature had no effect on plant biomass, physiological analyses revealed that combined elevated [CO_2] and temperature negatively affected photosynthetic performance. The limited energy levels resulting from the reduced respiratory and photorespiration rates of such plants were apparently inadequate to sustain nitrate reductase activity. Inhibited N assimilation was associated with a strong reduction in amino acid content, conditioned leaf soluble protein content and constrained leaf N status. Therefore, the plant response to elevated [CO_2] and elevated temperature resulted in photosynthetic acclimation. The reduction in transpiration rates induced limitations in nutrient transport in leaves of plants exposed to elevated [CO_2] and temperature, led to mineral depletion and therefore contributed to the inhibition of photosynthetic activity.

Abbreviations – ABA, abscisic acid; AQP, aquaporin; c-ZR, *cis*-zeatin riboside; DM, dry matter; DTT, dithiothreitol; GDH, glutamate dehydrogenase; GS, glutamine synthetase; HI, harvest index; HPLC-ES-MS/MS, high-performance liquid chromatography-electrospray-mass spectrometry; IAA, indole-3-acetic acid; iPR, isopentenyladenosine; NAD-GDH, glutamate dehydrogenase deamination; NADH-GDH, glutamate dehydrogenase amination; NR, nitrate reductase; NRT, nitrate transporter; PPFD, photosynthetic photon flux density; TGG, temperature gradient greenhouse; TOM, total organic matter; Tr, transpiration; TSP, total soluble protein; tZ, *trans*-zeatin.

Introduction

According to the Intergovernmental Panel on Climate Change (IPCC 2013), the carbon dioxide (CO_2) concentration has increased since the pre-industrial period from 280 to 400 parts per million (ppm). Current [CO_2] represents a record in the last 800 000 years. The different scenarios projected by the IPCC predict an increase in the atmospheric concentration that could reach 700 ppm by the end of the century (IPCC 2013). The increments in greenhouse gas emission will contribute toward increasing the ambient temperature by 2–6°C in Europe by 2100 and the expected warming is going to be greatest in summer in south-western Europe. More specifically, the European Environmental Agency has predicted an average rise of 4°C by 2080; likewise, extreme hot summers such as the heat wave experienced in Europe in 2003 are likely to become four times as common in Spain (and southern Europe). Therefore, global agricultural production will be greatly affected and these rapid changes signify critical uncertainty over food production (Loladze 2014, Myers et al. 2014). As Oury et al. (2012) attested for wheat production in France, climatic factors since the end of the 1980s have counterbalanced the genetic progress of recent decades. As a consequence, identification of wheat cultivars that will be better adapted to predicted climate change conditions is an important responsibility for plant science.

The effect of atmospheric [CO_2] on plant growth, and especially on photosynthetic performance, has been extensively studied during recent decades (Ainsworth et al. 2002, Aranjuelo et al. 2011, Long et al. 2004). It has been observed that after the initial stimulation of photosynthetic rates by elevated [CO_2] (Drake et al. 1997), these rates decline below their maximum potential; this is the process known broadly as photosynthetic acclimation (Ainsworth et al. 2004, Aranjuelo et al. 2013, Gutiérrez et al. 2009, Martínez-Carrasco et al. 2005). Additionally, as described by a number of authors (Bowes 1993, Drake and Leadley 1991, Long 1991, Morison and Lawlor 1999), CO_2 fixation is enhanced by increasing temperature. This phenomenon could be explained by an improvement in the utilization of photosynthetic end products through increased sink metabolism at elevated temperatures (Farrar and Williams 1991). Moreover, as reported by Long (1991), the kinetic parameters of Rubisco related to the relative solubility of CO_2 and O_2 suggest that the optimum temperature of photosynthesis will increase by several degrees in plant exposed to elevated [CO_2]. It has been suggested that the temperature at which CO_2 begins to have a positive effect on growth might be as high as 18.5°C and below that temperature, CO_2 enrichment might reduce growth (Idso et al. 1987). Some authors set the value at 8%°C^{-1} (Idso and Kimball 1989) while others suggest 2%°C^{-1} (Rawson 1992). However, other authors (Sage et al. 1995, Pérez et al. 2007, Aranjuelo et al. 2013, 2011a,) have found that the interaction of elevated CO_2 with high temperature reduces or eliminates the positive effect on plant production. These discrepancies may be because of the fact that above the optimum maximum, increases in temperature disable photosynthetic performance (Galmés et al. 2013). Therefore, the rate at which plants increase their response to CO_2 with increasing temperature is still unclear and needs to be revealed.

According to the source–sink hypothesis, the enhancement of leaf carbon concentrations, which is a consequence of the increase in plant photosynthetic rates under short-term exposure to elevated [CO_2], induces downregulation of genes encoding for the photosynthetic apparatus in order to balance sink capacity (Ainsworth et al. 2004, Long et al. 2004). Rubisco catalyzes the fixation of CO_2 and O_2 (photosynthesis and photorespiration, respectively), thus an increase in atmospheric [CO_2] will increase the leaf internal [CO_2] and the CO_2/O_2 ratio, which favors carboxylation rather than oxygenation (Andrews and Lorimer 1987). Sharkey (1988) calculated that doubling the present atmospheric [CO_2] would result in a 50% decrease in the ratio of photorespiration:photosynthesis. According to previous studies (Rachmilevitch et al. 2004, Bloom et al. 2014), elevated [CO_2]-derived inhibition of photorespiration would be linked to limitations in the nitrate assimilation capacity of plants. However, it should be considered that most of those findings are based on studies conducted under optimal growth conditions, while little is known about [CO_2] effect under elevated temperature conditions.

Although a large number of earlier studies have characterized the role of leaf N availability and the C sink/source balance during photosynthetic performance, there is still a limited understanding of the effects of elevated [CO_2] on nutrient translocation. Nutrient acquisition by plants is dependent on mass flow and diffusion (Matimati et al. 2014). Moreover, transpiration (Tr) is the dominant process that controls water transport in plants (Kramer and Boyer 1995). Because of the stomatal closure induced by elevated [CO_2], previous studies (Taub and Wang 2008, McGrath and Lobell 2013) have revealed that reduced Tr is involved in the lower shoot nutrient content of plants. Linked with this, aquaporins (AQPs) are central components in plant–water relations and nutrient transport at all levels of organization (cell, tissue, organ and whole plant). It is now widely known that most (75–95%) of the water transport is mediated by AQPs (Maurel 1997). Therefore, the open/closed state

of AQPs and their regulation are essential in maintaining cell water balance and nutrient transport within the plant.

Many experiments analyzing the effects of climate change on plant growth have considered the effect of CO_2 under optimal growth conditions. However, some uncertainty remains regarding the responsiveness of photosynthetic performance under elevated [CO_2] and the interaction of elevated [CO_2] with other environmental conditions, such as high temperature. In this experiment, wheat plants were grown at either 400 or 700 ppm [CO_2] and exposed to ambient or ambient + 4°C temperature during grain filling with the purpose of clarifying the potential mechanism involved in such response, in particular, photosynthetic performance and N metabolism. In order to elucidate this question, we proceeded to characterize leaf physiology, the metabolite profile (comprising the main soluble sugars, amino acids, starch and organic acids) together with the activity of enzymes and hormones involved in N assimilation. Moreover, in order to test the relevancy of the Tr stream in flag leaf nutrient composition, we characterized the expression of genes involved in ammonium (*AMP* 1), nitrate (*NRT* 1.1 and *NRT* 1.2) and water transport (*PIP* 1.1, *PIP* 1.2, *TIP* 1, *TIP* 2.1 and *TIP* 2.3). Moreover, plants were labeled with ^{15}N in order to determine N absorption.

Materials and methods

Plant material and experimental design

The experiment was conducted with high-yielding bread wheat (*Triticum durum,* var. 'Sula') plants. Seedlings were vernalized for a month at 4°C and later transplanted into 13-l pots (four plants per pot) containing a mixture of inert 2:2:1 (v/v/v) vermiculite/perlite/peat. The plants were transferred to the temperature gradient greenhouses (TGGs) with [CO_2] control located at the Universidad de Navarra campus (42.80°N, 1.66°W; Pamplona, Spain). Morales et al. (2014) described the design of these TGGs. Briefly, greenhouses are clear plastic, aluminum structure, box-shaped enclosures, 10.5 m long (including a 0.9 m outlet compartment), 2.2 m wide and 1.8 m high. The design included doors along the longitudinal walls which allowed access to plants inside. The CO_2 concentration was continuously monitored at the outlet module by an infrared gas analyzer whose signal was fed into a proportional, integrative, differential system controlling the opening time of a solenoid valve that injected CO_2. Ventilated temperature and humidity sensors (M22W2HT4X transmitters; Rotronic Instrument Corp., Hauppauge, NY, USA) and air probes connected to another CO_2 infrared gas analyzer were placed at the center of each module 60 cm above plants. Quantum sensors (Apogee SQ-200; Apogee Instruments Inc., Logan, UT, USA) were placed on top and inside of each tunnel to record photosynthetically active radiation. One group of plants was divided between two greenhouses where no [CO_2] was added and in which [CO_2] was maintained at ambient conditions (=400 μmol mol^{-1}). The other group of plants was transferred to two other greenhouses where the [CO_2] was increased to an elevated [CO_2] (=700 μmol mol^{-1}). Each tunnel was divided into three modules that provided different temperature values. The central module was regarded as a transition module and no experimental plants were included in it. In each tunnel, the inlet module was maintained at ambient temperature (20°C, T_{amb}) and the outlet module was maintained at this average ambient temperature + 4°C (T_{amb+4}). Terminal elevated temperature was selected because it is characteristic of regions with Mediterranean-type climates, where temperature increased in spring when wheat enters its reproductive stage (Fitzpatrick and Nix 1970). Plants were watered with a complete Hoagland solution twice a week and with water once a week to avoid excessive salt accumulation. When plants reached the ear emergence stage, half group of the plants within each TGG was moved from the ambient temperature modules to the elevated temperature modules.

In order to determine N absorption, ^{15}N labeling was conducted in half of the plants 2 weeks after they reached anthesis. N labeling was carried out by replacing the N in the Hoagland solution by ^{15}N-enriched $K^{15}NO_3$ (5%) for 5 days. After this exposure time, plants were harvested for later analysis of total organic matter (TOM) ^{15}N isotopic composition ($\delta^{15}N$) (see below). Plants were grown at the relevant [CO_2] and temperature conditions until they reached maturity.

Plant growth parameters

Eight plants per treatment combination were harvested at maturity. Collected samples were dried in an oven at 60°C for 48 h and afterwards dry matter (DM) was determined. The harvest index (HI) was calculated as the ratio between ear DM and total DM.

Gas exchange and chlorophyll fluorescence determinations

Developed and healthy flag leaves were selected to conduct gas exchange analyses using a LiCor 6400XP portable gas exchange photosynthesis system (LI-COR, Lincoln, NE, USA). Gas exchange analyses were determined in all the plants at 400 and 700 μmol mol^{-1} [CO_2] with a photosynthetic photon flux density (PPFD)

of 1200 µmol m^{-2} s^{-1}. The light-saturated rate of CO_2 assimilation (A_n) and intercellular [CO_2] (C_i) were estimated at a PPFD of 1200 µmol m^{-2} s^{-1}. Estimations of the maximum carboxylation velocity of Rubisco (Vc_{max}) were made using the method of Harley et al. (1992). The electron transport rate was calculated according to Krall and Edwards (1992) as $\Phi_{PSII} \times PPFD \times 0.84 \times 0.5$, where 0.5 was used as the fraction of the excitation energy distributed to PSII (Ogren and Evans 1993) and 0.84 as the fractional light absorbance (Morales et al. 1991). Dark respiration (R_D) measurements (carried out with the LiCor 6400XP gas exchange analyzer) were performed 30 min before the dark period started; measurements were made in automatic mode and therefore leaves were placed in the chamber for at least 10 min. The relative quantum efficiency of PSII photochemistry (Φ_{PSII}) was simultaneously measured with a fluorescence chamber (LFC 6400–40; Li-COR) coupled to the Li-Cor 6400 portable photosynthesis system. The rate of electron transport through PSII [Je(PSII)], electron flux for photosynthetic carbon reduction [Je(PCR)] and the electron flux for photorespiratory carbon oxidation [Je(PCO)] were measured as described by Epron et al. (1995).

Metabolite determinations

Soluble sugar, starch content and organic acids

Leaf extracts were homogenized with a solution containing ethanol 80% (v/v) that was sonicated for 25 min at 30°C using an Ultrasons-H (Selecta, Barcelona, Spain). The hydroalcoholic phase was evaporated through the Turbovap (Zymark, Carmel, IN, USA) and resuspended with 4 ml of distilled water. The sample was centrifuged at 2300 *g* for 10 min and the supernatant and the pellet were stored separately at −80°C.

Sucrose was determined in the supernatant fraction with a Beckman P/ACE5500 capillary electrophoresis system (Beckman Instruments, Fullerton, CA, USA) (Cabrerizo et al. 2001). Starch content was determined in the pellet according to the description of Aranjuelo et al. (2005).

Organic acids were determined in the supernatant fraction used for sugar analysis. The extracts were filtered with Milex filters (Millipore, Billerica, MA, USA) and injected in a DX-500 ion chromatograph equipped with an IonPac AS11 column connected to an ATC-1 protecting column and an AG11 precolumn (all chromatography equipment from Dionex, Salt Lake City, UT, USA).

Total amino acids and amino acid profile

Frozen plant tissue (0.1 g) was ground with liquid N_2 and homogenized with 1 ml of 1 *M* HCl. Then, the extract was centrifuged at 16 000 *g* and 4°C for 10 min. The pH of the supernatant was adjusted to 6.5–7 using NaOH and stored at −20°C. Amino acids were derivatized at room temperature between 12 and 16 h with fluorescein isothiocyanate (FITC) dissolved in 20 m*M* acetone/borate, pH 10. Single amino acids were determined by high-performance capillarity electrophoresis using a Beckman Coulter PA-800 apparatus (Beckman Coulter Inc., Brea, CA, USA) with laser-induced fluorescence detection (argon ion: 488 nm). Total amino acids were quantified as the sum of all individual amino acids obtained as detailed before.

TOM N isotope composition ($\delta^{15}N$)

Flag leaf blade samples collected on the last day of labeling were dried at 60°C for 48 h, and analyzed for the $\delta^{15}N$ of TOM. One milligram of ground sample was used for each determination. The $^{15}N/^{14}N$ ratios (R) of plant material were determined using an elemental analyzer (EA1108, Series 1, Carlo Erba Instrumentazione, Milan, Italy) coupled to an isotope ratio mass spectrometer (Delta C, Finnigan, Mat., Bremen, Germany) operating in continuous flow mode at the Scientific Service Facilities of the University of Barcelona (Spain).

The $^{15}N/^{14}N$ ratios of plant materials were also expressed in δ notation ($\delta^{15}N$) using international secondary standards of known $^{15}N/^{14}N$ ratios (IAEA N_1 and IAEA N_2 ammonium sulfate and IAEA NO_3 potassium nitrate) referred to N_2 in air, with analytical precision at about 0.2‰: $\delta^{15}N = \left(\frac{R_{sample}}{R_{standard}}\right) - 1$.

Carbon, nitrogen and mineral content

Carbon and nitrogen content were determined in dry samples previously ground to powder. One milligram samples were stored in tin capsules for TOM analyses. N and C content were determined at the Scientific Service Facilities of the University of Barcelona (Spain) using an elemental analyzer (EA1108, Series 1; Carbo Erba Instrumentazione, Milan, Italy).

The macronutrients potassium (K), calcium (Ca), phosphorus (P), sulfur (S) and magnesium (Mg) as well as the microelements iron (Fe), zinc (Zn), molybdenum (Mo), manganese (Mn), copper (Cu) and nickel (Ni) were determined after acid digestion using inductively coupled plasma/optical emission spectrometry (iCAP 6500 Duo; Thermo Fisher Scientific, Cambridge, UK).

Hormone content

The concentration of indole-3-acetic acid (IAA), abscisic acid (ABA), *trans*-zeatin (tZ), *cis*-zeatin riboside

(c-ZR) and isopentenyladenosine (iPR) in plants was analyzed in flag leaf extracts using high-performance liquid chromatography-electrospray-mass spectrometry (HPLC-ESI-MS/MS). The extraction and purification of these hormones were carried out using the following method: 0.25 g of frozen plant tissue (previously ground to a powder in a mortar with liquid N) was homogenized with 4 ml of precooled (−20°C) methanol:water:HCOOH (90:9:1, v/v/v with 2.5 m*M* sodium diethyldithiocarbamate). The deuterium-labeled internal standards [$^2H_5$-IAA (D-IAA), $^2H_6$-(+)-*cis*, *trans*-ABA (D-ABA) and tZ from OlChemin Ltd (Olomouc, Czech Republic), c-ZR from Sigma-Aldrich (St Louis, MO, USA) and iPR] were added to the extraction medium (20 µl of a stock solution of 2000 ng ml^{-1} of D-IAA and D-ABA in methanol). Extraction was performed by shaking the samples for 60 min at 2000 rpm at room temperature in a Multi Reax shaker (Heidolph Instruments, Schwabach, Germany). After extraction, solids were separated by centrifugation at 11 000 rpm for 10 min using a Centrikon T-124 centrifuge with an A8.24 rotor (Kontron Instruments, Cumbernauld, UK), and re-extracted by shaking for 20 min with an additional 3 ml of extraction mixture. Supernatants were passed through a Strata C18-E cartridge (3 cm, 200 mg) (Phenomenex, Torrance, CA, USA; Ref. 8B-S001-FBJ), preconditioned with 4 ml of methanol followed by 2 ml of extraction medium. After evaporation at 40°C until aqueous phase using a Labconco Vortex Evaporator (Labconco Co., Kansas City, MO, USA), 0.5 ml of 1 *M* formic acid was added. Hormones were then extracted with 5 ml of diethyl ether, and the organic phase was evaporated to dryness. The residue was redissolved in 250 µl of methanol/0.4% acetic acid (40:60, v/v) and centrifuged at 3750 g for 10 min before injection into the HPLC-ESI-MS/MS system.

Hormones were quantified by HPLC-ESI-MS/MS using an HPLC device (2795 Alliance HT; Waters Co., Milford, MA, USA) coupled to a 3200 Q TRAP LC/MS/MS System (Applied Biosystems/MDS Sciex, Ontario, Canada), equipped with an electrospray interface. A reverse-phase column (Synergi 4 mm Hydro-RP 80A, 150 × 2 mm; Phenomenex) was used. A linear gradient of methanol (A) and 0.4% acetic acid in water (B) was used: 35% A for 1 min, 35–60% for 5 min, 60–64% A for 8 min, 64–90% A for 1 min, 90% A for 1 min and 90–35% A for 1 min, followed by a stabilization time of 3 min. The flow rate was 0.20 ml min^{-1}, the injection volume was 40 µl and column and sample temperatures were 30 and 20°C, respectively. The detection and quantification of the hormones were carried out using multiple reaction monitoring in the negative-ion mode, employing multilevel calibration curves with the internal standards. Compound-dependent parameters are listed in Table 2. The source parameters are curtain gas: 22 psi, GS1: 45 psi, GS2: 55 psi, ion spray voltage: −4000 V and temperature: 550°C. Data samples were processed using ANALYST 1.4.2 Software from Applied Biosystems/MDS Sciex.

Enzymatic activities

NR activity

Nitrate reductase (NR) activity was measured according to Arrese-Igor et al. (1991). Leaf tissue (0.2 g) was ground to a powder in a mortar with liquid N and homogenized with the following extraction buffer (50 m*M* Mops-KOH, pH 7.8, 5 m*M* NaF, 1 µ*M* Na_2MoO_4, 10 µm flavin adenine dinucleotide (FAD), 2% polyvinylpolypyrrolidone (PVPP) 2 m*M* *β*-mercaptoethanol and 5 m*M* ethylenediaminetetraacetic acid (EDTA). The homogenate was centrifuged at 4°C for 5 min at 12 000 *g*. NR activity was measured immediately in the supernatant. The reaction mixture consisted of 50 m*M* Mops-KOH buffer, pH 7.5, supplemented with 1 m*M* NaF, 10 m*M* KNO_3, 0.17 m*M* NADH and either 10 m*M* $MgCl_2$ or 5 m*M* EDTA. The reaction was terminated after 8 or 16 min by the addition of an equal volume of sulfanilamide (1% in 3 *M* HCl) and then naphthylethylenediamine dihydrochloride (0.02%) to the reaction mixture, and the absorbance at 540 nm was measured. The activation state of NR was defined as the activity measured in the presence of 10 m*M* $MgCl_2$ divided by the activity measured in the presence of 5 m*M* EDTA (expressed as a percentage).

GS activity

Glutamate synthetase (GS) activity was measured according to Cruz et al. (2006). Leaf tissue (0.2 g) was ground to a powder in a mortar with liquid nitrogen and homogenized with the following extraction buffer: 50 m*M* Tris–HCl buffer (pH 8), 1 m*M* EDTA, 10 m*M* 2-mercaptoethanol, 5 m*M* dithiothreitol (DTT), 10 m*M* $MgSO_4$, 1 m*M* cysteine and 0.6% polyvinylpyrrolidone. The homogenate was filtered and centrifuged at 4°C for 15 min at 35 000 g and the supernatants were used for the assay. GS activity was assayed by the transferase reaction at 30°C in a medium containing 60 µmol imidazole, pH 7.0, 1 µmol $MnCl_2$, 6 µmol Na_2HAsO_4, 1.5 µmol ADP, 65 µmol glutamine, 50 µmol NH_2OH, pH 7.0 and enzyme in a total volume of 0.6 ml. The reaction was initiated by adding NH_2OH to the medium and stopped by adding 0.5 ml of 0.6 *M* $FeCl_3$ in 2.5 *M* HCl. Activity was assessed from absorbance determinations at 546 nm.

GDH activity

Glutamate dehydrogenase (GDH) was extracted by homogenizing 0.2 g of frozen tissue in 2 ml of 50 m*M* Tris–HCl buffer (pH 8) containing 1 m*M* EDTA, 10 m*M* 2-mercaptoethanol, 5 m*M* DTT, 10 m*M* $MgSO_4 \cdot 7H_2O$, 0.6% PVPP and 1 m*M* L-cysteine using an Ultra-Turrax T25 (Janke and Kunkel, Ika-Labortechnik, Staufen, Germany) for 15 s at 11000 g. The homogenates were centrifuged for 20 min at 3500 *g* at 4°C. Supernatants were collected and kept in ice for GDH assays.

GDH activity was determined in both the aminating (NADH-GDH) and the deaminating (NAD-GDH) directions by following the absorption change at 340 nm with a spectrophotometer (UV; Hewlett-Packard, San Diego, CA, USA). One unit of GDH activity was defined as the reduction or oxidation of 1 µmol of coenzyme (NAD or NADH, respectively) per min. The NADH forward (reductive amination) reaction was analyzed following the oxidation of NADH at 340 nm. The reaction mixture consisted of a 100 m*M* phosphate buffer (KH_2PO_4/K_2HPO_4; pH 7.5) containing α-ketoglutaric acid (25 m*M*), $(NH_4)_2SO_4$ (200 m*M*), NADH (1 m*M*) and 150 µl of crude enzyme extract in a 2 ml reaction assay. The GDH reaction was started by adding the NADH and its transformation to NAD^+ was followed at 340 nm in a UV spectrophotometer (UV; Hewlett–Packard). One international unit (IU) of enzyme activity is defined as the catalytic activity leading to the consumption of one micromole of NADH per min. The reverse reaction (oxidative deamination) assay was prepared by adding 100 m*M* tricine-KOH buffer (pH 8), 500 m*M* glutamate, 5 m*M* NAD^+ and 200 µl of crude enzyme extract in a 2 ml reaction assay. The reduction of NAD^+ was followed spectrophotometrically at 340 nm.

Gene expression

RNA isolation

Total RNA was isolated from flag leaves with a phenol/chloroform extraction method (Kay et al. 1987). DNase treatment of total RNA and cDNA synthesis was performed according to Qiagen's protocol (Quantitect Reverse Transcription KIT Cat#205311; Qiagen, CA, USA).

Quantitative real-time Reverse transcription polymerase chain reaction (RT-PCR)

The expression of each gene was studied by real-time PCR by using an iCycler (Bio-Rad, Hercules, CA, USA). cDNAs were obtained from 2.5 µg of total DNase-treated RNA in a 20 µl reaction containing oligo$(dT)_{15}$ primer (Promega, Madison, WI, USA), 10 m*M* dNTP (Invitrogen, Carlsbad, CA, USA), 0.1 *M* DTT (Invitrogen, Carlsbad, CA, USA), 40 U of RNase inhibitor (Promega), 5× first strand buffer (Invitrogen) and 200 U of Superscript II Reverse Transcriptase (Invitrogen) with the temperature recommended by the enzyme supplier. The primer sets used to amplify each studied gene in the synthesized cDNAs, including that of reference gene actin, are shown in Table S1.

Each 23 µl reaction contained 3 µl of a 1:10 dilution of the cDNA, 10.5 µl of Master Mix (Bio-Rad Laboratories S.A, Madrid, Spain), 8.6 µl of MilliQ H_2O and 0.45 µl of each primer pair. The PCR program consisted of a 3 min incubation at 95°C to activate the hot-start recombinant Taq DNA polymerase, followed by 31 cycles of 30 s at 94°C, 30 s at the established annealing temperature and 30 s at 72°C, where the fluorescence signal was measured, followed by 1 cycle of 1 min at 95°C, 1 min at 70°C and 60 cycles of 10 s at 70°C. The specificity of the PCR amplification procedure was checked with a heat dissociation protocol (from 70–100°C) after the final cycle of the PCR.

Real-time PCR experiments were carried out with four biological independent samples, with the threshold cycle (C_t) determined in triplicate. The relative levels of transcription were calculated by using the $2^{-\Delta\Delta Ct}$ method (Livak and Schmittgen 2001), using actin gene as reference with C_t variation among treatments less than 1. All the primers used presented efficiencies close to 1.9 as described by Pfaffl (2001). Negative controls without cDNA were used in all PCRs.

Statistical analyses

Statistical analysis was performed by two-factor ANOVA (SPSS v.12.0; SPSS Inc., Chicago, IL, USA). $[CO_2]$ treatment was selected as the first factor, whereas temperature was used as the second factor. The results were accepted as significant at $P < 0.05$. When differences between treatments were significant according to the ANOVA, least significant differences were evaluated using Tukey's b test ($P < 0.05$).

Results

Plant growth analyses (Table 1) showed that while total DM increased significantly under $[CO_2]$, temperature did not affect this parameter. Similar patterns were detected in the ear and shoot DM, and HI values (Table 1).

Gas exchange analyses (Fig. 1A) demonstrated that the effect of CO_2 on photosynthetic activity (A_n) was conditioned by temperature. While in ambient temperature the exposure to 700 µmol mol^{-1} increased A_n by

Table 1. Effect of elevated CO_2 (700 vs 400 μmol mol^{-1}) and temperature (Ambient, Amb vs elevated, Amb + 4°C) on total plant DM (Total DM, g plant^{-1}), ear DM (Total DM, g plant^{-1}), shoot DM (Total DM, g plant^{-1}) and HI (ear DM/plant DM) in Sula (*Triticum aestivum* L.) plants. Each value represents the mean ± SE of eight replications. Statistical analysis was made by a two-factor ANOVA. The different letters indicate significant differences ($P < 0.05$) between treatments as determined by Tukey b test.

Temperature	$[CO_2]$ (μmol mol^{-1})	Total DM	Ear DM	Shoot DM	HI
Amb	400	17.81 ± 1.99 b	6.36 ± 1.03 b	11.46 ± 1.65 a	35.82 ± 2.93 b
	700	28.04 ± 2.78 a	15.34 ± 1.34 a	11.34 ± 2.94 a	54.87 ± 4.29 a
Amb + 4°C	400	15.94 ± 1.54 b	7.15 ± 0.93 b	8.79 ± 1.65 b	44.57 ± 2.72 b
	700	23.42 ± 4.97 a	12.08 ± 2.00 a	12.70 ± 2.10 a	52.03 ± 3.76 a

42%, under elevated temperature conditions no significant effect was detected. Leaf Tr decreased in elevated $[CO_2]$; the lowest rate was found under elevated temperature (Fig. 1B). Intercellular $[CO_2]$ (C_i) increased under elevated $[CO_2]$ (Fig. 1C). Likewise, elevated $[CO_2]$ enhanced the Rubisco maximum carboxylation activity (Vc_{max}) in ambient temperature conditions, whereas it decreased when plants were exposed to elevated $[CO_2]$ and elevated temperature (Fig. 1D).

As shown in Fig. 2A, while temperature did not alter leaf photorespiration (R_L), its values decreased in plants exposed to 700 μmol mol^{-1} CO_2. Although dark respiration (R_D) was not affected by $[CO_2]$, it was diminished under elevated temperature (Fig. 1B). As shown in Fig. 3, under ambient temperature conditions, elevated $[CO_2]$ had no significant effect on total electron flux in terms of PSII [Je(PSII)] values. Nevertheless, exposure to elevated temperature conditions negatively affected this parameter because it was already enhanced by elevated temperature. Electron flux for photosynthetic carbon reduction [Je(PCR)] increased in elevated $[CO_2]$ when plants were grown under ambient temperature conditions; at the same time, no significant effect was observed in elevated temperature treatments because [Je(PCR)] was already enhanced by elevated temperature. (Fig. 3B). Finally, electron flux for photorespiratory carbon oxidation [Je(PCO)] was negatively affected by $[CO_2]$ (Fig. 3C) and the decline was more pronounced under elevated temperature.

Leaf carbohydrate content was modified in plants exposed to $[CO_2]$ and temperature treatments. As shown in Fig. 4, sucrose content was not modified by $[CO_2]$ exposure but was negatively affected by growing under elevated temperature conditions. Similar patterns were detected in starch content where exposure to 700 μmol mol^{-1} $[CO_2]$ did not significantly affect its availability while it was negatively affected by temperature increase (Fig. 4B). Fructose was not affected by either $[CO_2]$ or temperature. Glucose content was dependent on the combination of $[CO_2]$ and temperature treatment: under ambient temperature, elevated $[CO_2]$ decreased glucose availability while no effect was detected under elevated temperature. Concerning the leaf organic acid content, the data revealed that under ambient temperature and elevated $[CO_2]$ leaf malate content was reduced; however, under elevated temperature conditions, the increment in atmospheric $[CO_2]$ did not modify malate content (Fig. 4E). A similar pattern was found for oxaloacetate content (Fig. 4F), although elevated temperature alone diminished its levels. However, citrate content (Fig. 4G) was decreased in elevated $[CO_2]$ plants regardless of temperature.

Leaf mineral determinations showed that no significant differences were detected in C content and that in the case of N, significant depletion was detected only in plants exposed to elevated $[CO_2]$ and high temperature conditions (Table 2). Leaf total soluble protein was reduced under elevated $[CO_2]$ and this reduction was greater in plants under elevated temperature (Table 2). Interestingly, analysis of total amino acids revealed that temperature increased the amino acid content in plants exposed to 400 μmol mol^{-1} $[CO_2]$, whereas in treatments exposed to 700 μmol mol^{-1} $[CO_2]$, elevated temperature had a remarkable effect on total amino acid content, diminishing it by 95%, (Table 2). Although $\delta^{15}N$ determined in non-labeled plants (used as a control of $\delta^{15}N$ enrichment in ^{15}N-labeled plants) did not detect differences between treatments, elevated $[CO_2]$ diminished the $\delta^{15}N$ enrichment level, being more pronounced under elevated temperature (Table 2). The leaf amino acid content profile (Fig. 5) revealed that while glutamine, γ-Aminobutyric acid (GABA) and alanine decreased under ambient temperature and elevated $[CO_2]$ conditions, the amino acid levels (with the exception of GABA) were strongly reduced under elevated temperature conditions. Also, elevated temperature alone diminished Gln, GABA and Ala concentrations (Fig. 5).

Leaf macronutrient composition showed that although elevated $[CO_2]$ did not affect K, Ca, Mg, P and S availability under ambient temperature conditions, under high temperature conditions (with the exception of P) exposure to 700 μmol mol^{-1} decreased these values (Table 3). On the other hand, micronutrient analyses (Table 4)

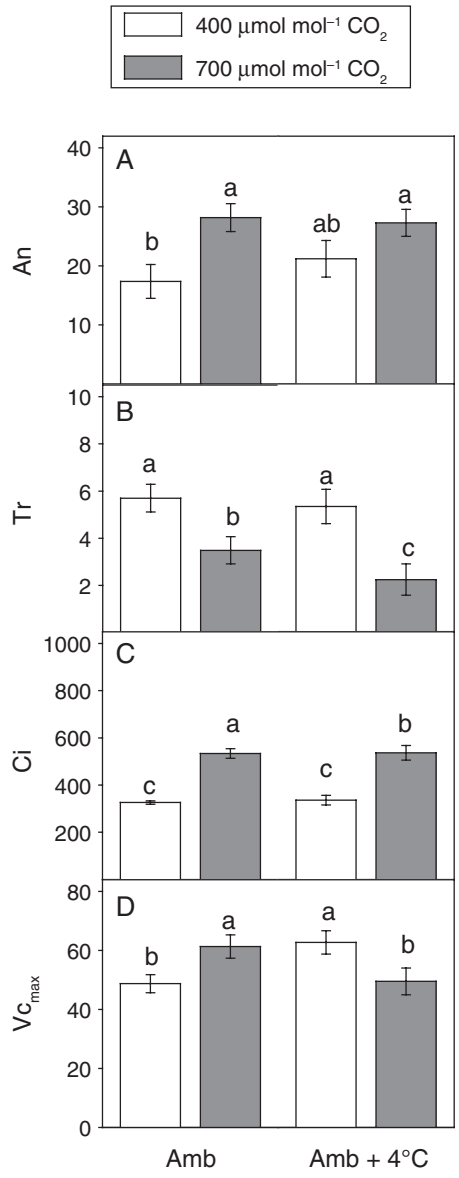

Fig. 1. Effect of elevated CO_2 (700 vs 400 µmol mol^{-1}) and temperature (Ambient, Amb vs elevated, Amb + 4°C) on flag leaf (A) net photosynthesis (A_n, µmol m^{-2} s^{-1}), (B) leaf Tr (mmol m^{-2} s^{-1}), (C) intercellular [CO_2] (C_i, µmol m^{-2} s^{-1}) and (D) Rubisco maximum carboxylation activity (Vc_{max}, mmol m^{-2} s^{-1}) in Sula wheat (*Triticum durum*, Def.) plants. Each value represents the mean ± SE of four replications. Statistical analysis was made by a two-factor ANOVA. The different letters above the columns indicate significant differences ($P < 0.05$) between treatments as determined by Tukey b test.

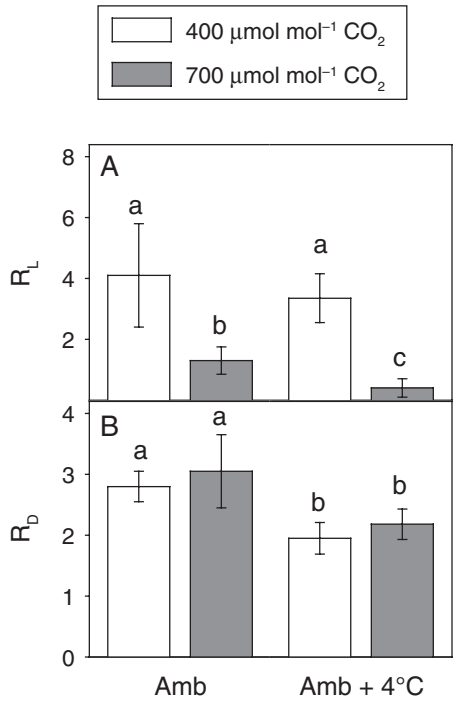

Fig. 2. Effect of elevated CO_2 (700 vs 400 µmol mol^{-1}) and temperature (Ambient, Amb vs elevated, Amb + 4°C) on (A) flag leaf photorespiration (R_L, µmol m^{-2} s^{-1}) and (B) dark respiration (R_D, µmol m^{-2} s^{-1}) in Sula wheat (*Triticum durum*, Def.) plants. Each value represents the mean ± SE of four replications. Statistical analysis was made by a two-factor ANOVA. The different letters above the columns indicate significant differences ($P < 0.05$) between treatments as determined by Tukey b test.

showed that, in general terms, elevated [CO_2] decreased Fe, Zn and Cu in both temperature treatments (Table 4).

Enzymatic activities involved in N assimilation displayed interesting results. Initial and maximum levels of NR (NR_{ini} and NR_{max}, respectively) decreased in wheat plants under elevated [CO_2] and elevated temperature conditions (Fig. 6A, B). However, no significant differences were observed in the NR activation state (NR_{activ}) (Fig. 6C). As shown in Fig. 6D, E, GDH amination (NADH-GDH) activity was negatively affected by elevated [CO_2] under elevated temperature conditions and GDH deamination (NAD-GDH) in ambient temperature treatments. Also, elevated temperature alone increased the NADH-GDH activity, but NAD-GDH activity decreased. Exposure to elevated [CO_2] stimulated GS activity in ambient temperature treatments (Fig. 6F); however, it was not modified under elevated temperature conditions.

Leaf hormone analyses (Table 5) highlighted that flag leaf IAA availability increased under elevated [CO_2] and ambient temperature, while it was decreased under elevated temperature. At the same time, ABA, cytokinins (CKs), iPR and c-ZR contents were decreased in plants exposed to elevated [CO_2] conditions, being more pronounced under elevated temperature for total CKs alone. Moreover, tZ diminished with 700 µmol mol^{-1} [CO_2] and elevated temperature.

Analysis of the gene expression of the plasma membrane intrinsic protein isoforms, *TaPIP*1.1 and TaPIP1.2,

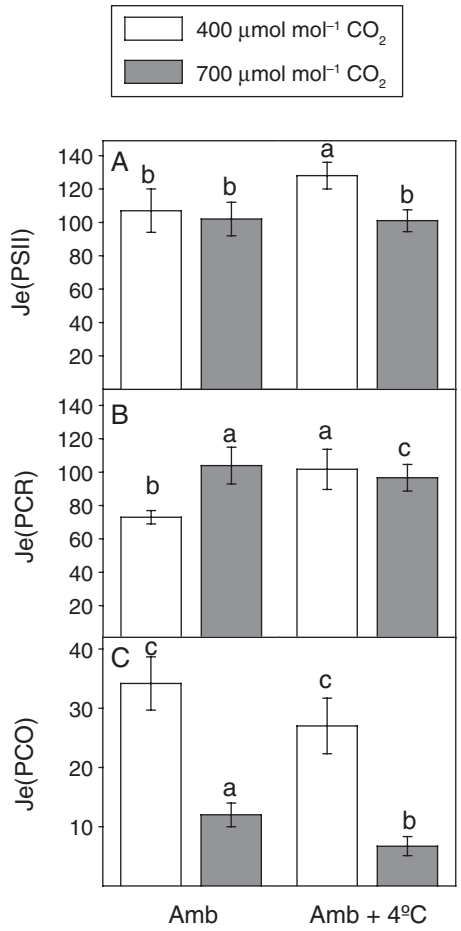

Fig. 3. Effect of elevated CO_2 (700 vs 400 µmol mol^{-1}) and temperature (Ambient, Amb vs elevated, Amb + 4°C) on (A) total electron flux in PSII [Je(PSII), µmol m^{-2} s^{-1}], (B) electron flux for photosynthetic carbon reduction [Je(PCR), µmol m^{-2} s^{-1}] and (C) electron flux for photorespiratory carbon oxidation [Je(PCO), µmol m^{-2} s^{-1}] in Sula wheat (*Triticum durum*, Def.) plants. Each value represents the mean ± SE of four replications. Statistical analysis was made by a two-factor ANOVA. The different letters above the columns indicate significant differences ($P < 0.05$) between treatments as determined by Tukey b test.

showed that although elevated [CO_2] reduced the expression of both isoforms under elevated temperature, only *TaPIP*1.2 gene expression was diminished under ambient temperature conditions (Fig. 7A, B). The gene expression of the tonoplast intrinsic protein isoform, *TaTIP*1 (Fig. 7C), and both *NRT*s (Fig. 7D, E) decreased under both elevated [CO_2] and elevated temperature conditions.

Discussion

It has been proposed that the expected increment in cereal production because of the rise in atmospheric [CO_2] (Amthor 1995, Manderscheid and Weigel 1995) may be reduced by the interaction of CO_2 with other limiting environmental factors, mainly temperature and low water and/or nitrogen availability (Aranjuelo et al. 2014, Lobell et al. 2011). As mentioned above, elevated temperature treatment was imposed during grain filling, coinciding with the period of greatest elevated temperature conditions in Mediterranean environments (Fitzpatrick and Nix 1970). Our study showed that although elevated [CO_2] increased total DM, its interaction with an increase of 4°C in ambient temperature counteracted the effect of the former on plant growth (Table 1). Absence of a temperature effect in the total DM could be because of the fact that (1) shoot biomass was formed in ambient temperature conditions and (2) grain filling is supported, to a large extent, by remobilization of C assimilated during the pre-anthesis period (Tambussi et al. 2007). Flag leaf photosynthesis also represents one of the major sources of C that sustains grain filling (Evans et al. 1975). The larger photosynthetic rates detected in plants exposed to 700 µmol mol^{-1} [CO_2] and ambient temperature suggested that, during grain filling, the CO_2 fixed during the post-heading period could have contributed to the increased ear DM (Fig. 1).

Previous studies (Escalona et al. 1999, Galmés et al. 2013) have determined that Rubisco activase activity is sensitive to raised temperature. Moreover, the decrease in Rubisco activity could have also been caused by its lower activation state (Pérez et al. 2007). While photosynthetic performance was not affected by elevated [CO_2] exposure under ambient temperature conditions (Aranjuelo et al. 2013), [CO_2] enhancement affected photosynthesis negatively in elevated temperature treatments (Fig. 1D). The Rubisco maximum carboxylation activity (Vc_{max}) showed that depleted Rubisco activity was involved in a lack of difference in the A_n of plants grown under elevated temperature conditions (Aranjuelo et al. 2005). As shown in Fig. 3, although exposure to 700 µmol mol^{-1} CO_2 and elevated temperature diminished the electron transport flux rate (JePSII), the fact that electron flux destined for photosynthetic carbon reduction (JePCR) was not modified allows us to discard electron availability as a factor involved in the depleted Vc_{max}. Therefore, Rubisco carboxylation inhibition might have been caused by a reduction in the total soluble protein concentration (Table 2) in plants exposed to elevated [CO_2] and elevated temperature (Pérez et al. 2011).

Classically, photosynthetic acclimation under elevated [CO_2] has been linked with limitations in increasing C sink strength: photosynthetic rates are decreased to balance C source activity and sink capacity (Ainsworth et al. 2004, Aranjuelo et al. 2013). During the grain filling period, ears represent a major C sink

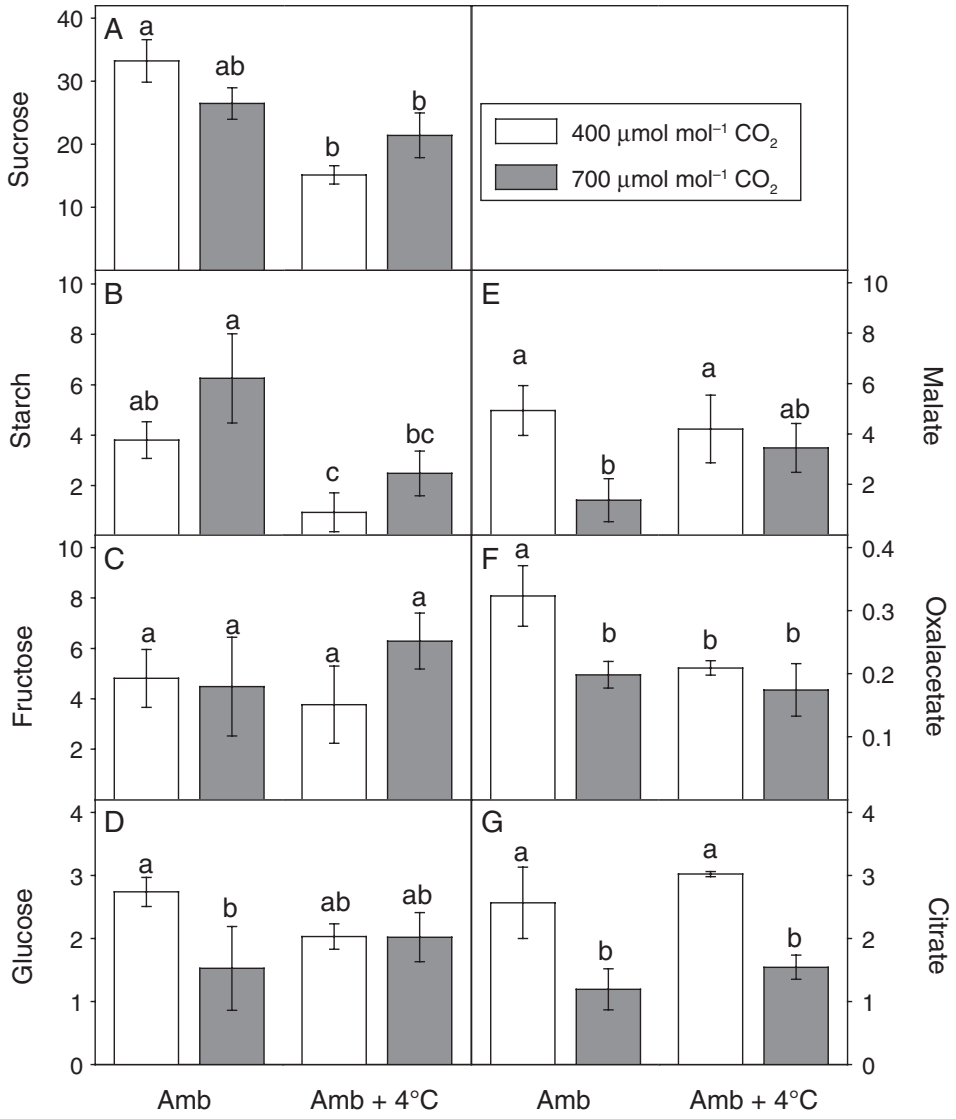

Fig. 4. Effect of elevated CO_2 (700 vs 400 µmol mol^{-1}) and temperature (Ambient, Amb vs elevated, Amb + 4°C) on flag leaf (A) sucrose (mg g^{-1}), (B) starch (mg g^{-1}), (C) fructose (mg g^{-1}), (D) glucose (mg g^{-1}), (E) malate (mg g^{-1}), (F) oxaloacetate (mg g^{-1}) and (G) citrate (mg g^{-1}) in Sula wheat (*Triticum durum*, Def.) plants. Each value represents the mean ± SE of four replications. Statistical analysis was made by a two-factor ANOVA. Values without a common letter above the columns are significantly different ($P < 0.05$) between treatments as determined by Tukey b test.

in plants (Tambussi et al. 2007). As shown in Table 1, regardless of the growth temperature, exposure to elevated [CO_2] increased ear DM (Aranjuelo et al. 2013). Leaf sucrose and starch content analyses (Fig. 4) highlighted the fact that under elevated temperature, plants remobilized a large part of the C present in starch in order to sustain the large C demand of grains during the filling period. Accordingly, total soluble sugars (TSS) and starch levels present in elevated [CO_2] treatments enabled carbohydrate imbalance to be discarded as a factor explaining the lower photosynthetic rates under enhanced temperature and [CO_2] conditions.

Plants exposed to elevated [CO_2] and temperature underwent reductions in leaf N content (Table 2). Decreases in N content have been widely described in plants exposed to [CO_2] (Cotrufo et al. 1998, Loladze 2014) and could be caused by the inhibition of leaf N assimilation because of the reduction in photorespiration rates (Rachmilevitch et al. 2004, Bloom et al. 2010, 2014). As shown in Fig. 1, photorespiration rates were more repressed under elevated [CO_2] and elevated temperature. Moreover, in these plants, we also detected a strong reduction in electron flux for photorespiratory carbon oxidation [Je(PCO)] (Fig. 3). As observed by

Table 2. Effect of elevated CO_2 (700 vs 400 μmol mol^{-1}) and temperature (Ambient, Amb vs elevated, Amb + 4°C) on flag leaf C (g 100 g^{-1}), leaf N (g 100 g^{-1}), leaf nitrate content (NO_3, μg g^{-1}), leaf total soluble protein (TSP, mg g^{-1}), total leaf amino acids content (μmol g^{-1}) and leaf N isotopic composition ($\delta^{15}N$, ‰) of ^{15}N non-labeled ($\delta^{15}N_{non\text{-}lab}$) and ^{15}N labeled ($\delta^{15}N_{lab}$) in Sula (*Triticum aestivum* L.) plants. Each value represents the mean ± SE of eight replications. Statistical analysis was made by a two-factor ANOVA. Values without a common letter indicate significant differences ($P < 0.05$) between treatments as determined by Tukey b test.

Temperature	[CO_2] (μmol mol^{-1})	C	N	NO_3	TSP	Total amino acid	$\delta^{15}N_{non\text{-}lab}$	$\delta^{15}N_{lab}$
Amb	400	45.87 ± 0.46 a	2.33 ± 0.33 a	23.19 ± 6.68 a	24.10 ± 4.29 a	13.62 ± 1.22 c	15.45 ± 0.64 a	543.63 ± 41.74 a
	700	45.91 ± 0.76 a	2.07 ± 0.28 ab	24.35 ± 8.87 a	19.41 ± 1.07 b	17.60 ± 0.95 b	14.16 ± 0.93 a	423.70 ± 18.35 b
Amb + 4°C	400	45.81 ± 0.89 a	2.36 ± 0.22 a	24.74 ± 8.64 a	23.78 ± 3.63 a	23.13 ± 0.82 a	14.27 ± 1.01 a	462.35 ± 23.84 ab
	700	46.20 ± 0.50 a	1.59 ± 0.34 b	22.73 ± 1.96 a	15.93 ± 2.17 c	0.94 ± 0.22 d	15.05 ± 0.70 a	362.62 ± 30.79 c

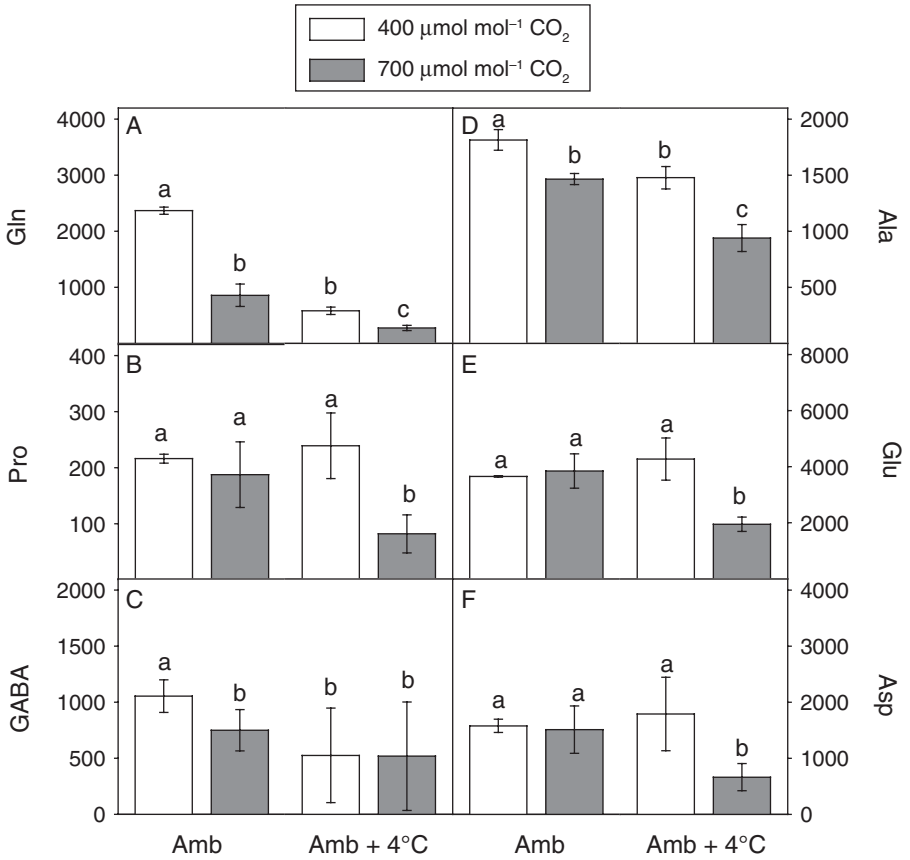

Fig. 5. Effect of elevated CO_2 (700 vs 400 μmol mol^{-1}) and temperature (Ambient, Amb vs elevated, Amb + 4°C) on flag leaf (A) glutamine (Gln, mg g^{-1}), (B) proline (Pro, mg g^{-1}), (C) GABA (mg g^{-1}), (D) alanine (Ala, mg g^{-1}), (E) glutamate (Glu, mg g^{-1}) and (F) aspartate (Asp, mg g^{-1}) in Sula wheat (*Triticum durum*, Def.) plants. Each value represents the mean ± SE of four replications. Statistical analysis was made by a two-factor ANOVA. Different letters above the columns indicate significant differences ($P < 0.05$) between treatments as determined by Tukey b test.

Rachmilevitch et al. (2004), reductions in the malate shuttle have been proposed as being involved in the inhibition of plant photorespiration under elevated [CO_2]. An absence of significant differences in malate content between temperature treatments of plants exposed to elevated [CO_2] could negate this hypothesis as an explanation for lower photorespiration and consequential inhibition of N assimilation. Limitations in energy availability have been linked to non-photorespiratory conditions (Foyer et al. 2012). Moreover, as observed by Eichelmann et al. (2011), several studies have elucidated the inhibitory effect of elevated temperature on plant respiration that contribute to limit the energy required for N assimilation. The reduction in dark respiration rates in plants exposed to elevated temperature (Fig. 1) suggests energy limitations. In addition, the reduction

Table 3. Effect of elevated CO_2 (700 vs 400 μmol mol^{-1}) and temperature (Ambient, Amb vs elevated, Amb + 4°C) on flag leaf macro-nutrient mineral content (g 100 g^{-1}) of K, Ca, Mg, P and S in Sula (*Triticum aestivum* L.) plants. Each value represents the mean ± SE of four replications. Statistical analysis was made by a two-factor ANOVA. Values without a common letter indicate significant differences ($P < 0.05$) between treatments as determined by Tukey b test.

Temperature	[CO_2] (μmol mol^{-1})	K	Ca	Mg	P	S
Amb	400	2.61 ± 0.36 a	0.35 ± 0.09 b	0.29 ± 0.06 b	0.18 ± 0.04 a	0.31 ± 0.07 ab
	700	1.65 ± 0.45 b	0.29 ± 0.07 b	0.33 ± 0.08 b	0.15 ± 0.03 a	0.29 ± 0.08 ab
Amb + 4°C	400	2.60 ± 0.28 a	0.58 ± 0.08 a	0.39 ± 0.04 a	0.13 ± 0.01 a	0.41 ± 0.11 a
	700	1.64 ± 0.33 b	0.39 ± 0.10 b	0.34 ± 0.09 b	0.12 ± 0.04 a	0.25 ± 0.04 b

Table 4. Effect of elevated CO_2 (700 vs 400 μmol mol^{-1}) and temperature (Ambient, Amb vs elevated, Amb + 4°C) on flag leaf micro-nutrient mineral content (mg kg^{-1}) of Fe, B, Mn, Zn, Cu and Mo in Sula (*Triticum aestivum* L.) plants. Each value represents the mean ± SE of four replications. Statistical analysis was made by a two-factor ANOVA. Values without a common letter indicate significant differences ($P < 0.05$) between treatments as determined by Tukey b test.

Temperature	[CO_2] (μmol mol^{-1})	Fe	B	Mn	Zn	Cu	Mo
Amb	400	61.71 ± 9.95 a	14.92 ± 3.85 b	127.94 ± 33.47 b	25.00 ± 3.10 a	5.47 ± 0.66 a	0.67 ± 0.12 b
	700	42.01 ± 6.76 b	26.99 ± 5.32 a	42.51 ± 9.52 c	12.76 ± 0.95 b	3.91 ± 0.47 b	0.91 ± 0.31 ab
Amb + 4°C	400	55.83 ± 19.24 ab	16.33 ± 4.85 b	184.81 ± 31.11 ab	24.16 ± 1.78 a	5.27 ± 0.80 a	0.69 ± 0.15 a
	700	32.73 ± 4.84 c	18.01 ± 3.79 b	202.40 ± 35.06 a	8.54 ± 1.46 c	3.73 ± 0.43 b	1.03 ± 0.34 b

in respiration found in this study is contrary to recent studies concluding that the rates of respiration were enhanced under elevated [CO_2] (Leakey et al. 2009, Watanabe et al. 2014). Therefore, our study highlights a possible energy limitation of wheat plants exposed to elevated temperature and elevated [CO_2]. In order to validate the possible reduction in leaf N assimilation, several enzymatic activities related to the nitrogen cycle were tested. Our study highlighted that under ambient temperature conditions, elevated [CO_2] did not modify NR activity (Fig. 6). Nevertheless, under elevated temperature conditions and elevated [CO_2], NR activity was strongly diminished (although the enzyme was activated). Likewise, although but to a lesser degree, a not significant decrease was observed in GS activity and a reduction in the GDH activity in plants exposed to elevated [CO_2] and elevated temperature. Likewise, determinations of GS and GDH activity reject their direct implication in the slight (not significant) reduction in leaf N content observed in photosynthetic performance under elevated [CO_2] and ambient conditions. Still, the N content was not affected, the depletion of NR and GS activities detected in plants exposed to elevated temperature and 700 μmol mol^{-1} [CO_2] caused the enormous inhibition of leaf total amino acid content (Table 1). Similarly, Lea et al. (2006) described that the deregulation of NR at the posttranscriptional level caused a huge reduction of amino acids content. More specifically, the substantial decrement in glutamine and glutamate (Fig. 4), as well as other N-related amino acids such as alanine and aspartic acid, strengthens the case for enzymatic activity inhibition under elevated [CO_2] and elevated temperature. It should be noted that the reduction in amino acid content is consistent with the decrement in protein content (Table 2) and depletion of enzymes involved in N assimilation such as NR and GS.

Photosynthetic rates might also be conditioned by limitations in CO_2 diffusion processes (Flexas et al. 2006, Galmés et al. 2013). The fact that the intercellular CO_2 concentration (Ci) values detected in plants under 700 μmol mol^{-1} CO_2 were higher in both temperature treatments discounts the idea that photosynthetic downregulation in wheat plants exposed to elevated [CO_2] and temperature may be because of the limitations in CO_2 conductance. Besides this, differences in C_i in leaves have been correlated with AQPs (Flexas et al. 2006). More specifically, PIP1.2 AQP (Fig. 7B) could be involved in CO_2 membrane diffusion as other PIP1 AQPs (Uehlein et al. 2012, Sade et al. 2014), which have lower expression in leaves in plants exposed to elevated [CO_2], regardless of the temperature treatment; there was an absence of differences in expression of PIP1.2 in plants under elevated [CO_2].

It is well known that plant responses to elevated [CO_2] leads to stomatal closure (Long et al. 2004). Such closure directly affects Tr rates, reduces water transport (Keenan et al. 2013) and therefore shortens mass flow of nutrients through the plant (McGrath and Lobell 2013). Consequently, it is likely that the depletion of leaf N content in plants exposed to elevated [CO_2] and elevated temperature (Table 2) could be because of N transport limitations. In our experiment, under elevated [CO_2] and elevated temperature, a lower Tr rate was detected, which correlated with a lower ^{15}N labeling level. As

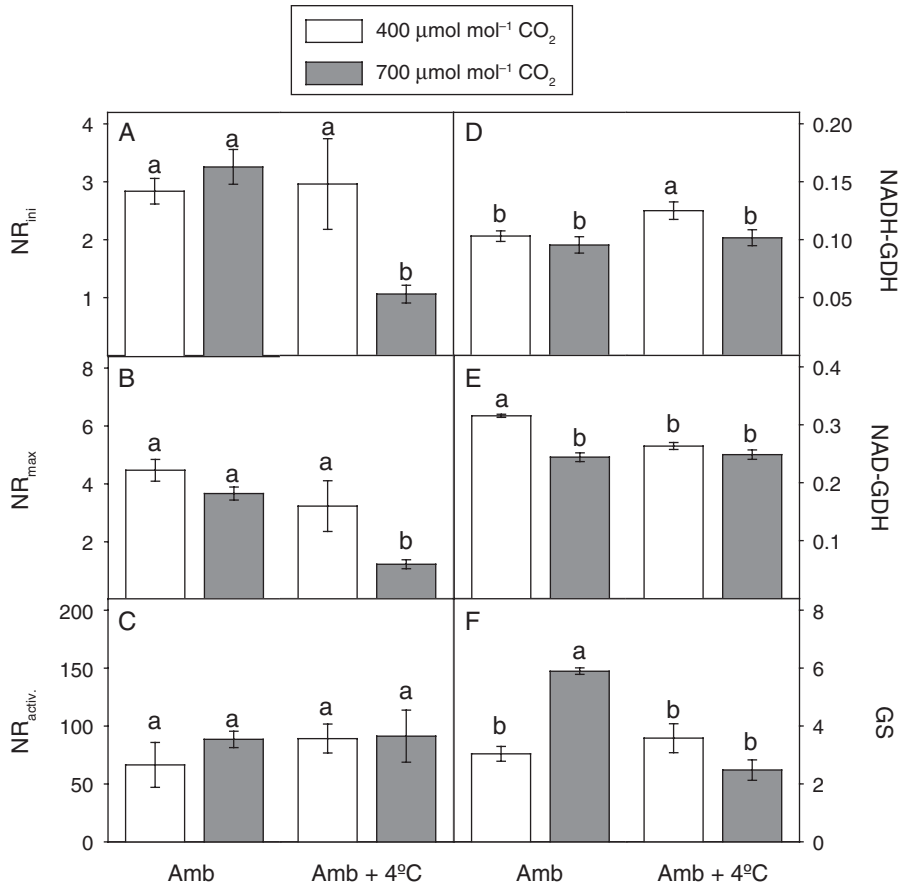

Fig. 6. Effect of elevated CO_2 (700 vs 400 µmol mol^{-1}) and temperature (Ambient, Amb vs elevated, Amb + 4°C) on flag leaf (A) NR initial (NR_{ini}, µmol g^{-1} h^{-1}), (B) maximal (NR_{max}, µmol g^{-1} h^{-1}), (C) activation state ($NR_{activ.}$, %), (D) NADH-GDH (µmol g^{-1} min^{-1}), (E) NAD-GDH (µmol g^{-1} min^{-1}) and (F) GS activity (µmol g^{-1} min^{-1}) in Sula wheat (*Triticum durum*, Def.) plants. Each value represents the mean ± SE of four replications. Statistical analysis was made by a two-factor ANOVA. Different letters above the columns indicate significant differences ($P < 0.05$) between treatments as determined by Tukey b test.

Table 5. Effect of elevated CO_2 (700 vs 400 µmol mol^{-1}) and temperature (Ambient, Amb vs elevated, Amb + 4°C) on flag leaf IAA, ABA, CKs and CK forms tZ, cZR and iPR content (pmol g^{-1}) in Sula (*Triticum aestivum* L.) plants. Each value represents the mean ± SE of four replications. Statistical analysis was made by a two-factor ANOVA. Different letters indicate significant differences ($P < 0.05$) between treatments as determined by Tukey b test.

Temperature	$[CO_2]$ (µmol mol^{-1})	IAA	ABA	CK	tZ	cZR	iPR
Amb	400	73.17 ± 15.81 b	30.21 ± 3.20 a	7.65 ± 0.96 a	1.54 ± 0.05 a	5.09 ± 1.19 a	1.03 ± 0.06 a
	700	135.99 ± 47.76 a	16.77 ± 2.94 b	3.41 ± 0.80 b	1.15 ± 0.11 a	1.80 ± 0.32 c	0.47 ± 0.04 b
Amb + 4°C	400	45.27 ± 2.78 c	33.63 ± 5.47 a	4.64 ± 1.38 b	1.56 ± 0.42 a	3.27 ± 0.94 b	0.80 ± 0.29 a
	700	40.76 ± 2.76 c	17.42 ± 2.47 b	1.98 ± 0.51 c	0.65 ± 0.05 b	1.07 ± 0.31 c	0.45 ± 0.16 b

shown in Table 2, the fact that the lowest $\delta^{15}N$ (during post-anthesis period) data were detected could be linked with a reduction in transport root-to-shoot. The repression of TIP1 AQP (Fig. 7C) and the diminution of ABA content (Table 5), both involved in leaf water conductance, were in line with this finding. Hence, the repression of the NRT 1.1 and 1.2 nitrate transporters under elevated $[CO_2]$ and elevated temperature suggests nitrate transport restrictions (Fig. 7). Hormones are another key factors involved in nutrient transport (Rubio et al. 2009). According to Sakakibara (2006), leaf N status is associated with the synthesis of CKs that act as N sensors because of their regulatory effect in the expression of genes involved in nutrient uptake. In this sense, elevation of both $[CO_2]$ and temperature could provoke an inhibitory effect through depletion of CKs (Table 5)

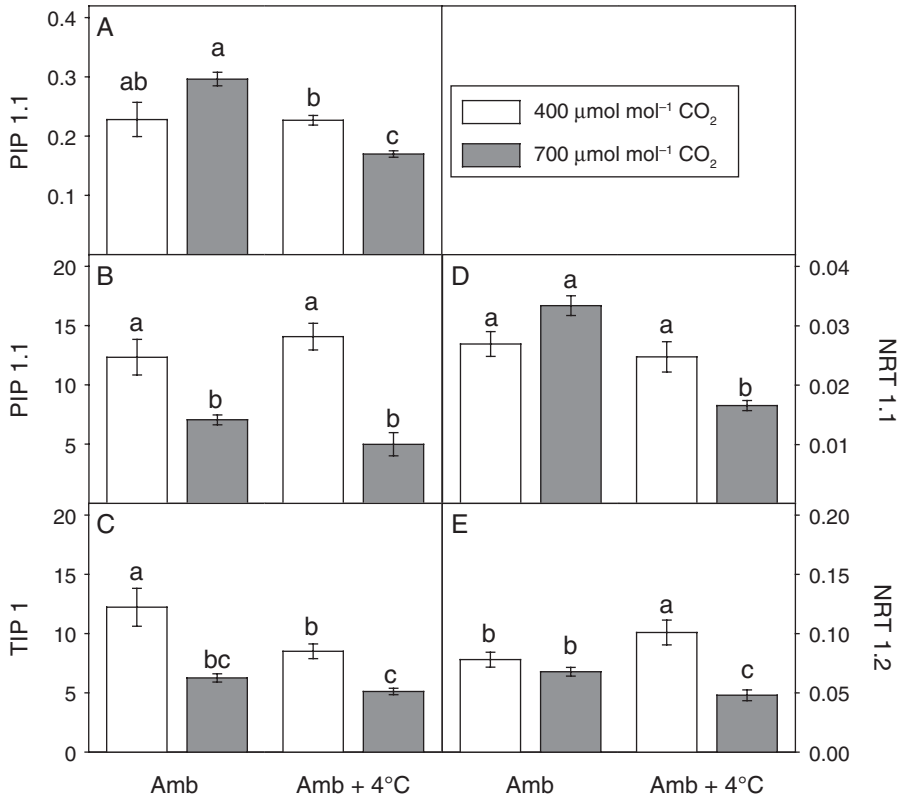

Fig. 7. Effect of elevated CO_2 (700 vs 400 µmol mol^{-1}) and temperature (Ambient, Amb vs elevated, Amb + 4°C) on the (A and B) expression of plasma membrane intrinsic proteins isoforms (PIP1.1 and PIP1.2), (C) tonoplast intrinsic protein isoforms (TIP 1) and (D and E) NRT (NRT 1.1 and NRT 1.2, respectively) genes in Sula wheat (*Triticum durum,* Def.) plants. Each value represents the mean ± SE of four replications. Statistical analysis was made by a two-factor ANOVA. Values without a common letter indicate significant differences ($P < 0.05$) between treatments as determined by Tukey b test.

and thus lead to impairment of N transport in plants. In addition, CK depletion was general for all CK forms (tZ, cZR and iPR) analyzed in wheat plants under elevated [CO_2] and temperature. Impaired nutrient uptake also conditioned the availability of other macro (K, Ca, Mg and S) and micro (Fe, Zn, Cu) elements (Tables 3 and 4) in plants exposed to elevated temperature and 700 µmol mol^{-1} [CO_2]. Similar depletions in the nutritional status of plants exposed to elevated [CO_2] have been described recently (Loladze 2014, Myers et al. 2014). At the physiological level, such systemic impoverishment is very relevant because it generates imbalances in plant mineral stoichiometry (Loladze 2002). In terms of Rubisco and chlorophyll, a reduction in Mg content under elevated [CO_2] has been proposed as a key response that underlines the importance of Tr rates and xylem flux in plant physiology (McGrath and Lobell 2013). Further, the decline in Ca under elevated [CO_2] has been reported previously (Duval et al. 2011, Loladze 2014) and has been linked with reductions in Tr rates observed in mutant *Arabidopsis* plants (Baxter 2009). Both Fe and Cu have been described as essential elements for photosynthesis, mitochondrial respiration and nitrogen metabolism (Hänsch and Mendel 2009), and Zn content has been linked to carbonic anhydrase content (Badger and Price 1994) and turnover of chloroplasts (Lu et al. 2011). Overall, these results highlight the fact that the lower mineral availability detected in this study, which was associated with a decline in Tr rates, could trigger N transport restrictions (as well as other minerals), and could therefore be the cause of the adverse photosynthetic performance observed in plants exposed to elevated [CO_2] and raised temperatures.

Conclusions

The results obtained in this study have highlighted the relevance of analyzing crop performance under interacting elevated [CO_2] and temperature. Regardless of the growth temperature, exposure to 700 µmol mol^{-1} increased biomass production. Nevertheless, physiological, metabolic and genomic analyses highlighted that

temperature increases had important implications in N assimilation and transport in plants. Depleted leaf photorespiration and dark respiration observed in elevated [CO_2] and temperature treatments revealed that there was less energy available for nitrate assimilation. Inhibited leaf nitrate assimilation was reflected in a strong inhibition of the amino acid content and conditioning of the leaf soluble protein content, and also negatively affected leaf N status, which all contributed to the photosynthetic acclimation of the plants. Moreover, the reduction in Tr rates could give rise to reductions in mineral transport under elevated temperature and [CO_2], manifesting in turn as limitations in mineral status that might diminish the photosynthetic machinery of plants.

Acknowledgements – This work has been funded by the Spanish National Research and Development Program (AGL2011-30386-C02-02 and AGL2013-44147-R). I. J. has been the holder of an FPI fellowship from the Spanish Ministry of Economy and Competitiveness. I. A. was the recipient of a Ramón y Cajal research grant (Spanish Economy and Competiveness Ministry). The authors would like to thank Amadeo Urdian and Héctor Santesteban for technical support with the CO_2 greenhouses and sample processing.

References

Ainsworth EA, Rogers A, Nelson R, Long SP (2004) Testing the "source–sink" hypothesis of down-regulation of photosynthesis in elevated [CO_2] in the field with single gene substitutions in *Glycine max*. Agric For Meteorol 122: 85–94

Ainsworth EA, Davey PA, Bernacchi CJ, Dermody OC, Heaton EA, Moore DJ, Morgan PB, Naidu SL, Ra HSY, Zhu XG, Curtis PS, Long SP (2002) A meta-analysis of elevated [CO_2] effects on soybean (*Glycine max*) physiology, growth and yield. Glob Chang Biol 8: 695–709

Amthor JS (1995) Terrestrial higher-plant response to increasing atmospheric [CO_2] in relation to the global carbon cycle. Glob Chang Biol 1: 243–274

Andrews JT, Lorimer GH (1987) Rubisco: structure, mechanisms and prospects for improvement. In: Hatch MD, Broadman NK (eds) Biochemistry of Plants, Vol. 10. Academic Press, New York, pp 132–207

Aranjuelo I, Irigoyen JJ, Perez P, Martinez-Carrasco R, Sanchez-Díaz M (2005) The use of temperature gradient tunnels for studying the combined effect of CO_2, temperature and water availability in N_2 fixing alfalfa plants. Ann Appl Biol 146: 51–60

Aranjuelo I, Cabrera-Bosquet L, Morcuende R, Avice J, Nogués S, Araus J, Martínez-Carrasco R, Pérez P (2011) Does ear C sink strength contribute to overcoming photosynthetic acclimation of wheat plants exposed to elevated CO_2? J Exp Bot 62: 3957–3969

Aranjuelo I, Sanz-Saez A, Jauregui I, Irigoyen JJ, Araus JL, Sánchez-Díaz M, Erice G (2013) Harvest index, a parameter conditioning responsiveness of wheat plants to elevated CO_2. J Exp Bot 64: 1879–1892

Aranjuelo I, Arrese-igor C, Molero G (2014) Nodule performance within a changing environmental context. J Plant Physiol 171: 1076–1090

Arrese-Igor C, Garcia-Plazaola JI, Diaz A, Aparicio-Tejo PM (1991) Distribution of nitrate reductase activity in nodulated lucerne plants. Plant Soil 131: 107–113

Badger MR, Price GD (1994) The role of carbonic anhydrase in photosynthesis. Annu Rev Plant Physiol Plant Mol Biol 45: 369–392

Baxter I (2009) Ionomics: studying the social network of mineral nutrients. Curr Opin Plant Biol 12: 381–386

Bloom AJ, Burger M, Asensio JSR, Cousins AB (2010) Carbon dioxide enrichment inhibits nitrate assimilation in wheat and *Arabidopsis*. Science 328: 899–903

Bloom AJ, Burger M, Kimball BA, Pinter PJ (2014) Nitrate assimilation is inhibited by elevated CO_2 in field-grown wheat. Nat Clim Change 4: 1758–6798

Bowes G (1993) Facing the inevitable: plants and increasing atmospheric CO_2. Annu Rev Plant Physiol Plant Mol Biol 44: 309–332

Cabrerizo PM, Gonzalez EM, Aparicio-Tejo PM, Arrese-Igor C (2001) Continuous CO_2 enrichment leads to increased nodule biomass, carbon availability to nodules and activity of carbon-metabolising enzymes but does not enhance specific nitrogen fixation in pea. Physiol Plant 113: 33–40

Cotrufo MF, Ineson P, Scott A (1998) Elevated CO_2 reduces the nitrogen concentration of plant. Glob Chang Biol 4: 43–54

Cruz C, Bio FM, Domínguez-Valdivia MD, Aparicio-Tejo PM, Lamsfus C, Martins-Loução MA (2006) How does glutamine synthetase activity determine plant tolerance to ammonium? Planta 223: 1068–1080

Drake BG, Leadley PW (1991) Canopy photosynthesis of crops and native plant communities exposed to long-term elevated CO_2. Plant Cell Environ 14: 853–860

Drake BG, González-Meler MA, Long SP (1997) More efficient plants: a consequence of rising atmospheric CO_2? Annu Rev Plant Physiol Plant Mol Biol 48: 609–639

Duval BD, Blankinship JC, Dijkstra P, Hungate B (2011) CO_2 effects on plant nutrient concentration depend on plant functional group and available nitrogen: a meta-analysis. Plant Ecol 213: 505–521

Eichelmann H, Oja V, Peterson RB, Laisk A (2011) The rate of nitrite reduction in leaves as indicated by O_2 and CO_2 exchange during photosynthesis. J Exp Bot 62: 2205–2215

Epron D, Godard D, Cornic G, Genty B (1995) Limitation of net CO_2 assimilation rate by internal resistances to CO2 transfer in the leaves of two tree species (*Fagus sylvatica* L. & *Castanea sativa* Mill.). Plant Cell Environ 18: 43–51

Escalona JM, Flexas J, Medrano H (1999) Stomatal and nonstomatal limitations of photosynthesis under water stress in field-grown grapevines. Aust J Plant Physiol 26: 421–433

Evans LT, Wardlaw IF, Fischer RA (1975) Crop Physiology; Some Case Histories. Cambridge University Press, Cambridge

Farrar JF, Williams ML (1991) The effects of increased atmospheric carbon dioxide and temperature on carbon partitioning, source–sink relations and respiration. Plant Cell Environ 14: 819–830

Fitzpatrick EA, Nix HA (1970) The climatic factor in Australian grassland ecology. In: Moore RM (ed) Australian Grasslands. Australian National University Press, Canberra, pp 3–26

Flexas J, Ribas-Carbó M, Hanson DT, Bota J, Otto B, Cifre J, McDowell N, Medrano H, Kaldenhoff R (2006) Tobacco aquaporin NtAQP1 is involved in mesophyll conductance to CO_2 in vivo. Plant J 48: 427–439

Foyer CH, Neukermans J, Queval G, Noctor G, Harbinson J (2012) Photosynthetic control of electron transport and the regulation of gene expression. J Exp Bot 63: 1637–1661

Galmés J, Aranjuelo I, Medrano H, Flexas J (2013) Variation in Rubisco content and activity under variable climatic factors. Photosynth Res 117: 73–90

Gutiérrez E, Gutiérrez D, Morcuende R, Verdejo AL, Kostadinova S, Martinez-Carrasco R, Pérez P (2009) Changes in leaf morphology and composition with future increases in CO_2 and temperature revisited: wheat in field chambers. J Plant Growth Regul 28: 349–357

Hänsch R, Mendel RR (2009) Physiological functions of mineral micronutrients (Cu, Zn, Mn, Fe, Ni, Mo, B, Cl). Curr Opin Plant Biol 12: 259–266

Harley PC, Loreto F, Di Marco G, Sharkey TD (1992) Theoretical considerations when estimating the mesophyll conductance to CO_2 flux by analysis of the response of photosynthesis to CO_2. Plant Physiol 98: 1429–1436

Idso SB, Kimball BA, Anderson MG, Mauney JR. (1987) Effects of atmospheric CO_2 enrichment on plant growth: the interactive role of air temperature. Agric Ecosyst Environ 20: 1–10

Idso SB, Kimball BA (1989) Growth response of carrot and radish to atmospheric CO_2 enrichment. Environ Exp Bot 29: 135–139

IPCC (2013) Summary for policymakers. In: Stocker TF, Qin D, Plattner G-K., Tignor M, Allen SK, Boschung J, Nauels A, Xia Y, Bex V, Midgley PM (eds) Climate Change 2013 – The Physical Science Basis. Working Group I Contribution to the Fifth Assessment Report of the Intergovernmental Panel on Climate Change. Cambridge University Press, Cambridge, pp 1–27.

Kay R, Chan A, Daly M, McPherson J (1987) Duplication of CaMV 35S promoter sequences creates a strong enhancer for plant genes. Science 236: 1299–1302

Krall JP, Edwards GE (1992) Relationship between photosystem II activity and CO_2 fixation in leaves. Physiol Plant 86: 180–187

Keenan TF, Hollinger DY, Bohrer G, Dragoni D, Munger JW, Schmid HP, Richardson AD (2013) Increase in forest water-use efficiency as atmospheric carbon dioxide concentrations rise. Nature 499: 324–327

Kramer PJ, Boyer JS (1995) Water Relations of Plants and Soils. Academic Press, New York

Lea U, Leydecker M, Quilleré I (2006) Posttranslational regulation of nitrate reductase strongly affects the levels of free amino acids and nitrate, whereas transcriptional regulation has only minor influence. Plant Physiol 140: 1085–1094

Leakey ADB, Ainsworth EA, Bernacchi CJ, Rogers A, Long SP, Ort DR (2009) Elevated CO_2 effects on plant carbon, nitrogen, and water relations: six important lessons from FACE. J Exp Bot 60: 2859–2876

Livak KJ, Schmittgen TD (2001) Analysis of relative gene expression data using real-time quantitative PCR and the 2-DDCt method. Methods 25: 402–408

Lobell DB, Schlenker W, Costa-Roberts J (2011) Climate trends and global crop production since 1980. Science 333: 616–620

Loladze I (2002) Rising atmospheric CO_2 and human nutrition: toward globally imbalanced plant stoichiometry? Trends Ecol Evol 17: 457–461

Loladze I (2014) Hidden shift of the ionome of plants exposed to elevated CO_2 depletes minerals at the base of human nutrition. eLIFE: 1–29. DOI:10.7554/eLife.02245

Long SP (1991) Modification of the response of photosynthetic productivity to rising temperature by atmospheric CO_2 concentration: has its importance been underestimated? Plant Cell Environ 14: 729–739

Long SP, Ainsworth EA, Rogers A, Ort DR (2004) Rising atmospheric carbon dioxide: plants FACE the future. Annu Rev Plant Biol 55: 591–628

Lu Y, Savage LJ, Larson MD, Wilkerson CG, Last RL (2011) Chloroplast 2010: a database for large-scale phenotypic screening of *Arabidopsis* mutants. Plant Physiol 155: 1589–1600

Manderscheid R, Weigel HJ (1995) Do increasing atmospheric CO_2 concentrations contribute to yield increases of German crops? J Agron Crop Sci 175: 73–82

Martínez-Carrasco R, Pérez P, Morcuende R (2005) Interactive effects of elevated CO_2, temperature and

nitrogen on photosynthesis of wheat grown under temperature gradient tunnels. Environ Exp Bot 54: 49–59
Matimati I, Verboom GA, Cramer MD (2014) Nitrogen regulation of transpiration controls mass-flow acquisition of nutrients. J Exp Bot 65: 159–168
Maurel C (1997) Aquaporins and water permeability of plant membranes. Annu Rev Plant Physiol Plant Mol Biol 48: 399–429
McGrath JM, Lobell DB (2013) Reduction of transpiration and altered nutrient allocation contribute to nutrient decline of crops grown in elevated CO_2 concentrations. Plant Cell Environ 36: 697–705
Morales F, Abadía A, Abadía J (1991) Chlorophyll fluorescence and photon yield of oxygen evolution in iron-deficient sugar beet (*Beta vulgaris* L.) leaves. Plant Physiol 97: 886–893
Morales F, Pascual I, Sánchez-Díaz M, Aguirreolea J, Irigoyen JJ, Goicoechea N, Antolín MC, Oyarzun M, Urdiain A (2014) Methodological advances: using greenhouses to simulate climate change scenarios. Plant Sci 226: 30–40
Morison JIL, Lawlor DW (1999) Interactions between increasing CO_2 concentration and temperature on plant growth. Plant Cell Environ 22: 659–682
Myers SS, Zanobetti A, Kloog I, Huybers P, Leakey ADB, Bloom AJ, Carlisle E, Dietterich LH, Fitzgerald G, Hasegawa T, Holbrook NM, Nelson RL, Ottman MJ, Raboy V, Sakai H, Sartor K, Schwartz J, Seneweera S, Tausz M, Usui Y (2014) Increasing CO_2 threatens human nutrition. Nature 510: 139–142
Ögren E, Evans JR (1993) Photosynthetic light-response curves. 1. The influence of CO_2 partial pressure and leaf inversion. Planta 189: 182–190
Oury F, Godin C, Mailliard A, Chassin A, Gardet O, Giraud A, Heumez E, Morlais J, Rolland B, Rousset M, Trottet M, Charmet G (2012) A study of genetic progress due to selection reveals a negative effect of climate change on bread wheat yield in France. Eur J Agron 40: 28–38
Pérez P, Zita G, Morcuende R, Martínez-Carrasco R (2007) Elevated CO_2 and temperature differentially affect photosynthesis and resource allocation in flag and penultimate leaves of wheat. Photosynthetica 45: 9–17
Pérez P, Alonso A, Zita G, Morcuende R, Martínez-Carrasco R (2011) Down-regulation of Rubisco activity under combined increases of CO_2 and temperature minimized by changes in Rubisco kcat in wheat. Plant Growth Regul 65: 439–447
Pfaffl MW (2001) A new mathematical model for relative quantification in real-time RT-PCR. Nucleic Acids Res: 29, e45
Rachmilevitch S, Cousins AB, Bloom AJ (2004) Nitrate assimilation in plant shoots depends on photorespiration. Proc Natl Acad Sci USA 101: 11506–11510
Rawson HM (1992) Plant responses to temperature under conditions of elevated CO_2. Aust J Bot 40: 473–490
Rubio V, Bustos R, Irigoyen ML, Cardona-López X, Rojas-Triana M, Paz-Ares J (2009) Plant hormones and nutrient signaling. Plant Mol Biol 69: 361–373
Sade N, Shatil-Cohen A, Attia Z, Maurel C, Boursiac Y, Kelly G, Granot D, Yaaran A, Lerner S, Moshelion M (2014) The role of plasma membrane aquaporins in regulating the bundle sheath-mesophyll continuum and leaf hydraulics. Plant Physiol 166: 1609–1620
Sage RF, Šantrucek J, Grise DJ (1995) Temperature effects on the photosynthetic response of C_3 plants to long-term CO_2 enrichment. Vegetatio 121: 67–77
Sakakibara H (2006) Cytokinins: activity, biosynthesis, and translocation. Annu Rev Plant Biol 57: 431–439
Sharkey TD (1988) Estimating the rate of photorespiration in leaves. Physiol Plant 73: 147–152
Tambussi EA, Bort J, Guiamet JJ, Nogues S, Araus JL (2007) The photosynthetic role of ears in C3 cereals: metabolism, water use efficiency and contribution to grain yield. Crit Rev Plant Sci 26: 1–16
Taub DR, Wang X (2008) Why are nitrogen concentrations in plant tissues lower under elevated CO_2? A critical examination of the hypotheses. J Integr Plant Biol 50: 1365–1374
Uehlein N, Otto E, Eilingsfeld A, Itel F, Meier W, Kaldenhoff R (2012) Gas-tight triblock-copolymer membranes are converted to CO_2 permeable by insertion of plant aquaporins. Sci Rep 2: 538
Watanabe CK, Sato S, Yanagisawa S, Uesono Y, Terashima I, Noguchi K (2014) Effects of elevated CO_2 on levels of primary metabolites and transcripts of genes encoding respiratory enzymes and their diurnal patterns in *Arabidopsis thaliana*: possible relationships with respiratory rates. Plant Cell Physiol 55: 341–357

Edited by C. Foyer